

A new search for the $K_L \rightarrow \pi^0 \nu \bar{\nu}$ and $K_L \rightarrow \pi^0 X^0$ decays

J-PARC KOTO collaboration

J. K. Ahn¹, K. Y. Baek², S. Banno³, B. Beckford⁴, B. Brubaker^{5,18}, T. Cai^{5,19}, M. Campbell⁴, C. Carruth^{4,20}, S. H. Chen⁶, S. Chu⁵, J. Comfort⁷, Y. T. Duh⁶, T. Furukawa⁸, H. Haraguchi³, T. Hineno⁹, Y. B. Hsiung⁶, M. Hutcheson⁴, T. Inagaki¹⁰, M. Ise³, E. Iwai^{3,21}, T. Kamibayashi¹¹, I. Kamiji⁹, N. Kawasaki⁹, E. J. Kim¹², Y. J. Kim¹³, J. W. Ko¹³, T. K. Komatsubara^{10,22}, A. S. Kurilin^{14,23}, G. H. Lee¹², H. S. Lee¹⁵, J. W. Lee^{3,24}, S. K. Lee¹², G. Y. Lim^{10,22}, C. Lin⁶, J. Ma⁵, Y. Maeda^{9*,25}, T. Masuda^{9,26}, T. Matsumura¹⁶, D. Mcfarland⁷, J. Micallef^{4,27}, K. Miyazaki³, K. Morgan^{5,28}, R. Murayama³, D. Naito^{9,29}, K. Nakagiri⁹, Y. Nakajima^{9,30}, Y. Nakaya^{3,23}, H. Nanjo^{9,31}, T. Nomura^{10,22}, T. Nomura¹¹, Y. Odani⁸, R. Ogata⁸, H. Okuno¹⁰, T. Ota⁸, Y. D. Ri³, M. Sasaki¹¹, N. Sasao¹⁷, K. Sato^{3,30}, T. Sato¹⁰, S. Seki⁹, T. Shimogawa^{8,29}, T. Shinkawa¹⁶, S. Shinohara⁹, K. Shiomi^{3,32}, J. S. Son¹², J. Stevens^{7,33}, S. Su⁴, Y. Sugiyama^{3,29}, S. Suzuki⁸, Y. Tajima¹¹, G. Takahashi⁹, Y. Takashima³, M. Tecchio⁴, I. Teo^{5,34}, M. Togawa³, T. Toyoda³, Y. C. Tung^{6,35}, T. Usuki⁹, Y. W. Wah⁵, H. Watanabe^{10,22}, N. Whallon^{4,36}, J. K. Woo¹³, J. Xu⁴, M. Yamaga^{3,37}, S. Yamamoto⁸, T. Yamanaka³, H. Yamauchi⁸, Y. Yanagida³, H. Yokota¹⁶, H. Y. Yoshida¹¹, and H. Yoshimoto³

¹Department of Physics, Korea University, Seoul 02841, Republic of Korea

²Department of Physics, Pusan National University, Busan 46241, Republic of Korea

³Department of Physics, Osaka University, Toyonaka, Osaka 560-0043, Japan

⁴Department of Physics, University of Michigan, Ann Arbor, MI 48109, USA

⁵Enrico Fermi Institute, University of Chicago, Chicago, IL 60637, USA

⁶Department of Physics, National Taiwan University, Taipei, Taiwan 10617, Republic of China

⁷Department of Physics, Arizona State University, Tempe, AZ 85287, USA

⁸Department of Physics, Saga University, Saga 840-8502, Japan

⁹Department of Physics, Kyoto University, Kyoto 606-8502, Japan

¹⁰Institute of Particle and Nuclear Studies, High Energy Accelerator Research Organization (KEK), Tsukuba, Ibaraki 305-0801, Japan

¹¹Department of Physics, Yamagata University, Yamagata 990-8560, Japan

¹²Division of Science Education, Chonbuk National University, Jeonju 54896, Republic of Korea

¹³Department of Physics, Jeju National University, Jeju 63243, Republic of Korea

¹⁴Laboratory of Nuclear Problems, Joint Institute for Nuclear Researches, Dubna, Moscow reg. 141980, Russia

¹⁵RISP, Institute for Basic Science, Daejeon 34047, Republic of Korea

¹⁶Department of Applied Physics, National Defense Academy, Kanagawa 239-8686, Japan

¹⁷Research Institute for Interdisciplinary Science, Okayama University, Okayama 700-8530, Japan

¹⁸Present address: Department of Physics, Yale University, New Haven, CT 06520-8120, USA

¹⁹Present address: Department of Physics and Astronomy, University of Rochester, Rochester, NY 14627-0171, USA

²⁰Present address: Department of Physics, University of California at Berkeley, Berkeley, CA 94720-7300, USA

²¹Present address: Department of Physics, University of Michigan, Ann Arbor, MI 48109, USA

²²Also at J-PARC Center, Tokai, Ibaraki 319-1195, Japan

²³Deceased

²⁴Present address: Department of Physics, Korea University, Seoul 02841, Republic of Korea

²⁵Present address: Kobayashi-Maskawa Institute, Nagoya University, Nagoya 464-8602, Japan

²⁶Present address: Research Institute for Interdisciplinary Science, Okayama University, Okayama 700-8530, Japan

²⁷Present address: Department of Physics and Astronomy, Michigan State University, East Lansing, MI 48824, USA

²⁸Present address: Department of Physics, University of Wisconsin-Madison, Madison, WI 53706-1390, USA

²⁹Present address: Accelerator Laboratory, High Energy Accelerator Research Organization (KEK), Tsukuba, Ibaraki 305-0801, Japan

³⁰Present address: Kamioka Observatory, Institute for Cosmic Ray Research, University of Tokyo, Kamioka, Gifu 506-1205, Japan

³¹Present address: Department of Physics, Osaka University, Toyonaka, Osaka 560-0043, Japan

³²Present address: Institute of Particle and Nuclear Studies, High Energy Accelerator Research Organization (KEK), Tsukuba, Ibaraki 305-0801, Japan

³³Present address: Department of Physics, Cornell University, Ithaca, NY 14853-2501, USA

³⁴Present address: Department of Physics, University of Illinois at Urbana-Champaign, Urbana, IL 61801-3080, USA

³⁵Present address: Enrico Fermi Institute, University of Chicago, Chicago, IL 60637, USA

³⁶Present address: Department of Physics, University of Washington, Seattle, WA 98195-1560, USA

³⁷Present address: Controls and Computing Division, Japan Synchrotron Radiation Research Institute (JASRI), Hyogo 679-5198, Japan

*E-mail: maeda_y@scphys.kyoto-u.ac.jp

.....
We searched for the CP -violating rare decay of neutral kaon, $K_L \rightarrow \pi^0 \nu \bar{\nu}$, in data from the first 100 hours of physics running in 2013 of the J-PARC KOTO experiment. One candidate event was observed while 0.34 ± 0.16 background events were expected. We set an upper limit of 5.1×10^{-8} for the branching fraction at the 90% confidence level (C.L.). An upper limit of 3.7×10^{-8} at the 90% C.L. for the $K_L \rightarrow \pi^0 X^0$ decay was also set for the first time, where X^0 is an invisible particle with a mass of $135 \text{ MeV}/c^2$.
.....

Subject Index C03, C30

1. *Introduction* The rare decay $K_L \rightarrow \pi^0 \nu \bar{\nu}$ of the long-lived neutral kaon is a direct CP -violating process [1, 2], and is one of the most sensitive probes to search for new physics beyond the standard model (SM) of particle physics. Because this decay proceeds through the flavor changing neutral current via the $s \rightarrow d$ transition, it is strongly suppressed in the SM and is sensitive to new heavy particles contributing to the decay [3, 4]. The SM predicts the branching fraction (Br) to be $(3.00 \pm 0.30) \times 10^{-11}$ [5], while the current experimental upper limit is 2.6×10^{-8} at the 90% confidence level (C.L.) set by the KEK E391a experiment [6]. The BNL E949 experiment [7] has set an indirect and model-independent limit $\text{Br}(K_L \rightarrow \pi^0 \nu \bar{\nu}) < 1.46 \times 10^{-9}$ based on the measurement of the $K^+ \rightarrow \pi^+ \nu \bar{\nu}$ branching fraction [8].

The signature of the $K_L \rightarrow \pi^0 \nu \bar{\nu}$ decay is a single π^0 from a K_L decay in flight without any other detectable particles. The experimental study is also sensitive to the two-body decay $K_L \rightarrow \pi^0 X^0$, where X^0 is an invisible boson. It was recently pointed out that the limit 1.46×10^{-9} based on the K^+ measurement does not apply to the $K_L \rightarrow \pi^0 X^0$ decay if the mass of X^0 is close to the π^0 mass and new physics with a weakly-interacting light particle can be probed through the $K_L \rightarrow \pi^0 \nu \bar{\nu}$ study [9, 10].

The KOTO experiment [11] at the Japan Proton Accelerator Research Complex (J-PARC) [12] is the successor of E391a, which was the first dedicated search for $K_L \rightarrow \pi^0 \nu \bar{\nu}$. KOTO adopts the same experimental techniques and aims at a sensitivity of 10^{-11} by adding a new beam line and various improvements of the detector. This letter reports the results from the first physics data collected in May 2013.

2. *Apparatus* The experiment was conducted at the Hadron Experimental Facility (HEF) [13] of J-PARC. A beam of 30-GeV protons was slowly extracted from the Main Ring (MR) accelerator [14] onto a 66-mm-long gold target [15] at HEF. The K_L 's produced at an angle of 16° direction from the proton beam were transported through a neutral beam line [16, 17] consisting of two collimators made of iron and tungsten, a sweeping magnet, and a 7-cm-thick lead photon absorber. The solid angle of the neutral beam after collimation was $7.8 \mu\text{sr}$, and its size was $8 \times 8 \text{ cm}^2$ at 20 m downstream from the target. The peak K_L momentum was $1.4 \text{ GeV}/c$. The beam also contained neutrons and photons. Neutrons outside the nominal beam solid angle, which came from scattering inside the collimators, are referred to as “halo neutrons.”

A schematic view of the detector is shown in Fig. 1. The 3-m-long decay volume along the beam direction was inside the detector. Two photons from a π^0 decay were detected by the electromagnetic calorimeter. It consisted of 2716 undoped CsI crystals, stacked inside a 1.9-m-diameter cylinder except the central $20 \times 20 \text{ cm}^2$ region. The size of each crystal within (outside) the central $1.2 \times 1.2 \text{ m}^2$ region was $2.5 \times 2.5 \text{ cm}^2$ ($5.0 \times 5.0 \text{ cm}^2$) in cross section and 50 cm in length, which corresponded to 27 radiation lengths in the beam direction. The energy resolution of the calorimeter was evaluated as $\sigma_E/E = (0.99 \oplus 1.74/\sqrt{E})\%$, where \oplus indicates a quadratic sum, and E is in GeV [18]. Details of the calorimeter are described in Refs. [19, 20]. Subsystems other than the calorimeter in the KOTO detector were “veto counters,” which ensured that no other detectable particles were emitted in the K_L decay. The gaps between the cylinder and the crystals of the calorimeter were filled with lead-scintillator sandwich counters named OEV [21]. The beam hole of $15 \times 15 \text{ cm}^2$ was located at the center of the calorimeter to let the beam particles pass through. The hole was surrounded with counters named LCV and CC03, which were composed of plastic scintillator plates and CsI crystals, respectively. The upstream surface of the calorimeter was covered with the Charged Veto (CV) counter [22], consisting of two layers of 3-mm-thick plastic scintillator sheets, to veto the K_L decays with charged particles. The outside region of the decay volume was surrounded by the Main Barrel (MB) [23]. The MB was a sandwich-type shower counter with lead and plastic scintillator sheets, and detected extra particles from the $K_L \rightarrow 3\pi^0$ and $K_L \rightarrow 2\pi^0$ decays. A counter of plastic scintillator sheets, named BCV, covered the inner surface of MB. The upstream end of the decay region was covered by the Front Barrel (FB) [23] and the Neutron Collar Counter (NCC) [24]. The FB was a lead-scintillator sandwich counter and NCC was made of CsI crystals. These veto counters detected photons from K_L decays in the upstream direction. The downstream region of the calorimeter was covered by a series of photon veto counters named CC04, CC05 and CC06, and in-beam counters named BHCV and BHPV [25]. They were meant to detect particles escaping in the forward direction through the beam hole of the calorimeter. Counters except for CC05, CC06, BHCV, and BHPV were located in vacuum at 0.1 Pa, and the decay volume was kept at $5 \times 10^{-5} \text{ Pa}$ to suppress π^0 's produced by the interactions of neutrons in the beam with residual gas. This

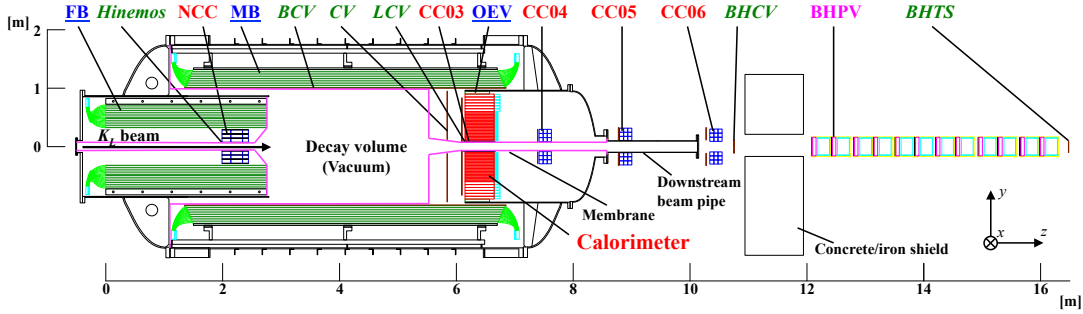


Fig. 1 Cut-out-view of the KOTO detector assembly in the physics run of May 2013. Veto counters with their names written in blue underlined, green italic and red regular letters are made of lead-scintillator sandwich, plastic scintillator and undoped CsI crystal, respectively. The downstream counter named as BHPV is made of lead-aerogel sandwich. The Hinemos and BHTS counters were used only for background studies and calibration, but not for veto.

high vacuum region was separated from the counter region with a multi-layer film called “membrane,” whose area density was $202 \mu\text{g}/\text{cm}^2$.

Signals from the calorimeter and the veto counters were recorded as waveforms to separate multiple overlapping hits. For most detectors, 125-MHz waveform digitizers [26] were used after shaping the raw pulses to Gaussian-like pulses with $\sigma \sim 30$ ns. For the in-beam counters, whose counting rates reached an order of MHz, 500-MHz digitizers [27] without pulse shaping were used.

3. *Data taking* The data analyzed in this letter was collected in 100 hours between May 19 and 23, 2013, before the data taking was suspended due to an incident at HEF caused by an accelerator malfunction [28]. The beam power incident on the gold target was 24 kW, which corresponded to 3×10^{13} protons on target (POT) in a 2-second-long duration (spill) with a 6 second repetition. The total number of POT was 1.6×10^{18} . The data acquisition system was triggered by two levels of trigger logic [29]. The first level trigger (L1) required the total energy detected in the calorimeter to be larger than 550 MeV. The acceptance loss due to this and the subsequent offline requirement was less than 1%. It also required the total energy deposition to be less than 1 MeV in CV and less than 50-60 MeV in NCC, MB, and CC03 to reject most of K_L decays with charged particles or photons hitting the veto counters. The energy thresholds for the L1 selection were set to be looser than those for the offline analysis. In the second level trigger (L2), the center of energy deposition (COE) in the calorimeter was calculated and the distance from the beam center to the COE position was required to be larger than 165 mm. This requirement was used to suppress the $K_L \rightarrow 3\pi^0$ decay because the energy of photons from the decay will balance in the transverse direction, while the COE distance tends to be large in the $K_L \rightarrow \pi^0\nu\bar{\nu}$ decay due to the neutrinos in the final state. With these trigger requirements, 300 million events were collected for $K_L \rightarrow \pi^0\nu\bar{\nu}$. To collect data from the $K_L \rightarrow 3\pi^0$, $K_L \rightarrow 2\pi^0$, and $K_L \rightarrow 2\gamma$ decays simultaneously for normalization and calibration purposes, disregarding the L2 decision, events which satisfied the L1 requirements, and L1 requirements without

veto were also recorded with prescaling factors of 30 and 300, respectively. In total, ~ 8000 events per spill were collected.

4. *Reconstruction and selection* At first, photon candidates in the calorimeter were reconstructed. After requiring an energy deposit larger than 3 MeV to identify hits in a single crystal, a cluster of hits in adjacent crystals was associated to an electromagnetic shower generated by a photon as described in Ref. [30]. After the photon reconstruction, events with two photons were selected for π^0 reconstruction. The π^0 -decay vertex position (Z_{vtx}) was obtained assuming that a $\pi^0 \rightarrow 2\gamma$ decay occurred on the beam (z) axis. Here, the z axis is defined as the center of the beam as shown in Fig. 1 and $z = 0$ m corresponds to 21.5 m downstream from the target. The transverse momentum (P_T) and the decay time of the π^0 were calculated with the calorimeter information and Z_{vtx} .

A series of event selection criteria (cuts) was imposed on the reconstructed π^0 kinematics and the hit information of the veto counters. To ensure the L1 and L2 requirements of the calorimeter in the offline analysis were met, the sum of the two photon energies was required to be larger than 650 MeV, and the COE position was required to be farther than 200 mm from the beam center. Events were rejected if any channel in the veto counters had a hit coincident with the π^0 decay time. Timings in most of the veto counters were calculated by using the pulse shape near the peak; with this method, possible errors in the timing evaluations due to overlapping multiple pulses, which could give a detection inefficiency, was reduced. The typical energy thresholds for the veto cuts were 2-3 MeV for the photon veto counters and 0.2 MeV for CV to achieve tight rejection to both the extra photons and charged particles in the K_L decay. The shape of the cluster in the x - y plane was required to be consistent with the expected shape of an electromagnetic shower due to a single photon obtained by simulation [18]. This requirement rejected events containing a cluster made by multiple photons or a hadronic shower made by neutrons. We also developed neural network cuts to further remove neutron contributions, based on the difference of kinematic features and cluster shapes between photon and neutron in the calorimeter. Details on the selection criteria are described in Ref. [31].

We set the signal region for the $K_L \rightarrow \pi^0 \nu \bar{\nu}$ decay using the P_T and Z_{vtx} of the reconstructed π^0 . The P_T was required to be larger than 150 MeV/ c to remove $K_L \rightarrow \pi^+ \pi^- \pi^0$ events for which the π^0 is restricted to have a transverse momentum less than 133 MeV/ c [33]. To avoid contaminations from halo neutron interactions with detectors, we also required $3000 < Z_{\text{vtx}} < 4700$ mm. The probability that a K_L entering the KOTO detector decays in this Z_{vtx} region was 3.2%. The events observed in this analysis are shown in Fig. 2, in which all the cuts except for P_T and Z_{vtx} have been imposed. To avoid introducing bias in the cut optimization, all criteria were pre-determined before examining events in and around the signal region, indicated by the box with a thin solid line in Fig. 2.

5. *Background estimation* Table 1 summarizes the estimation of background events in the signal region. The numbers of observed events and estimated background events inside and outside of the signal region are also shown in Fig. 2. The backgrounds were categorized into two types: K_L backgrounds and neutron backgrounds.

The K_L backgrounds were evaluated by using Geant4-based [32] Monte Carlo simulations (MC) for each K_L decay mode. Accidental hits in the KOTO detector had been collected

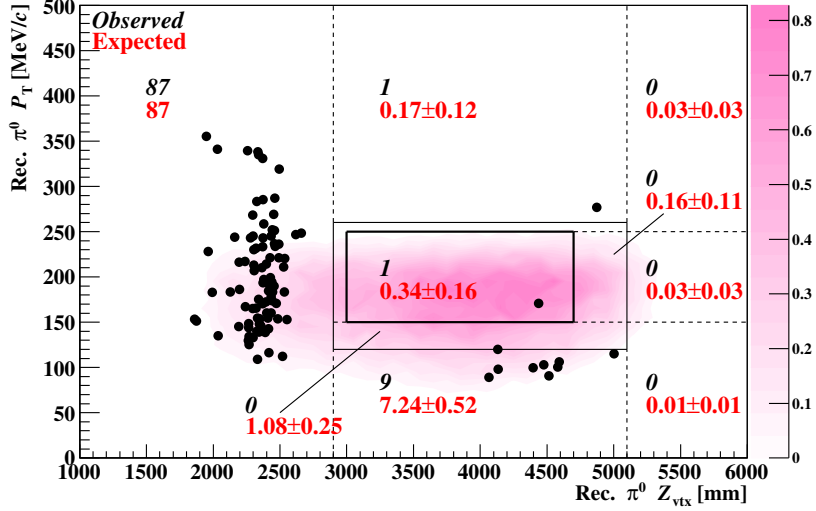


Fig. 2 Reconstructed π^0 transverse momentum (P_T) versus decay vertex position (Z_{vtx}) of the events with all the analysis cuts imposed. The region surrounded with a thick solid line is the signal region. The black dots represent the data, and the contour indicates the distribution of the $K_L \rightarrow \pi^0 \nu \bar{\nu}$ decay from MC. The events in the region surrounded with a thin solid line were not examined before the cuts were finalized. The black italic (red regular) numbers indicate the numbers of observed events (expected background events) for the regions divided by solid and dashed lines.

simultaneously with the data taking, and were overlaid to the MC samples. The background studies based on MC were validated with the $K_L \rightarrow 2\pi^0$ and $K_L \rightarrow 3\pi^0$ data. To reconstruct the $K_L \rightarrow 2\pi^0$ ($K_L \rightarrow 3\pi^0$) decays, events with four (six) photons in the calorimeter were selected. Among all possible combinations of the photons, the combination that had the best agreement of the Z_{vtx} values for two (three) π^0 's was adopted. Figure 3 shows the four-photon invariant mass distribution of the $K_L \rightarrow 2\pi^0$ events before and after imposing the veto cuts. The events in the low mass region are mostly from the $K_L \rightarrow 3\pi^0$ decays in which four out of six photons were detected in the calorimeter. The reduction of these events by detecting the extra two photons in the veto counters is well reproduced by the MC. Figure 4 shows the distributions of the reconstructed K_L decay vertex position and energy of the $K_L \rightarrow 3\pi^0$ events, which indicated the acceptance derived from MC was well understood.

The $K_L \rightarrow 2\pi^0$ decay is the major K_L background source because there are only two extra photons which can be detected by veto counters. We generated a MC sample with 40-times the statistics of the data. With two MC events that remained in the signal region after imposing all the cuts, the background contribution was estimated to be 0.047 events. For other decay modes, we generated the MC samples with various assumptions of topologies or mechanisms that could cause backgrounds to $K_L \rightarrow \pi^0 \nu \bar{\nu}$. In the case of $K_L \rightarrow \pi^+ \pi^- \pi^0$, for instance, the decay can be a background if charged pions hit the downstream beam pipe, which was made of 5-mm-thick stainless steel, and were undetected. The nine events located in the low- P_T region ($P_T < 120$ MeV/c, $2900 < Z_{\text{vtx}} < 5100$ mm) in Fig. 2 are explained by this mechanism. The requirement $P_T > 150$ MeV/c reduced the $K_L \rightarrow \pi^+ \pi^- \pi^0$ background to a negligible level. The $K_L \rightarrow 2\gamma$ decay can be a background if an incident K_L is scattered

Table 1 Summary of background estimation in the signal region.

background source	number of events
$K_L \rightarrow 2\pi^0$	0.047 ± 0.033
$K_L \rightarrow \pi^+\pi^-\pi^0$	0.002 ± 0.002
$K_L \rightarrow 2\gamma$	0.030 ± 0.018
pileup of accidental hits	0.014 ± 0.014
other K_L background	0.010 ± 0.005
halo neutrons hitting NCC	0.056 ± 0.056
halo neutrons hitting the calorimeter	0.18 ± 0.15
total	0.34 ± 0.16

at the upstream vacuum window, which was made of 125- μm -thick polyimide film, and obtains a finite transverse momentum. The $K_L \rightarrow 2\gamma$ decay was simulated for K_L 's with the transverse momentum larger than 20 MeV/ c , and the number of this background was estimated to be 0.03 events. Accidental hits overlapping with the $K_L \rightarrow \pi^\pm e^\mp \nu_e$, $K_L \rightarrow \pi^\pm \mu^\mp \nu_\mu$, $K_L \rightarrow 3\pi^0$, and $K_L \rightarrow \pi^+\pi^-\pi^0$ decays can change the reconstructed hit timing and cause an inefficiency. The background due to this inefficiency was separately treated and estimated to be 0.014 events.

The neutron backgrounds were caused by halo neutrons. One type of neutron background came from halo neutrons interacting with the NCC detector material in the upstream end of the decay volume. Secondary particles by such interactions were detected by the calorimeter and mimicked the π^0 from the $K_L \rightarrow \pi^0 \nu \bar{\nu}$ decay. The events in the upstream region ($Z_{\text{vtx}} < 2900$ mm) in Fig. 2 are π^0 's produced by this process. They can be a background when photon energies are mismeasured or a secondary neutron is detected in the calorimeter and misidentified as a photon. The contribution due to this mechanism was estimated with the MC, in which the halo neutrons were generated by a beam-line simulation and its yield was normalized to the number of the upstream events in the data. We evaluated this background to be 0.056 events.

Another type of the neutron background was due to halo neutrons hitting directly the calorimeter. A neutron incident on the calorimeter can deposit energy through hadronic interactions, and a secondary neutron from these interactions can deposit energy at another place after traveling inside the calorimeter. The contribution due to this mechanism was estimated with the data from a special run with a 5-mm-thick aluminum plate inserted inside the beam at $z = 2795$ mm. Neutrons in the beam scattered at the plate would hit the calorimeter and mimic the background events. We used the events which remained inside the signal region in this special run to estimate the number of background events. This sample was also used for training the neural network used for making cuts in the analysis. This background, estimated to be 0.18 events, was found to be the main background source in this analysis.

Details on the background estimation are described in Ref. [31]. The total number of expected background events was 0.34 ± 0.16 .

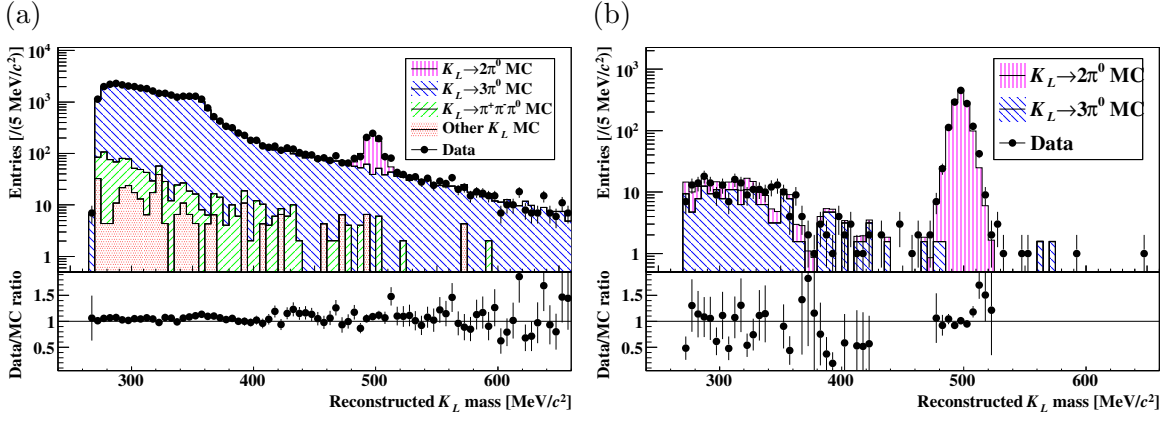


Fig. 3 Distributions of four-photon invariant mass of the $K_L \rightarrow 2\pi^0$ events before (a) and after (b) imposing the veto cuts. The dots with error bars are for data, and colored histograms are for MC. The bottom regions in both panels show the ratio of data and MC events for each histogram bin.

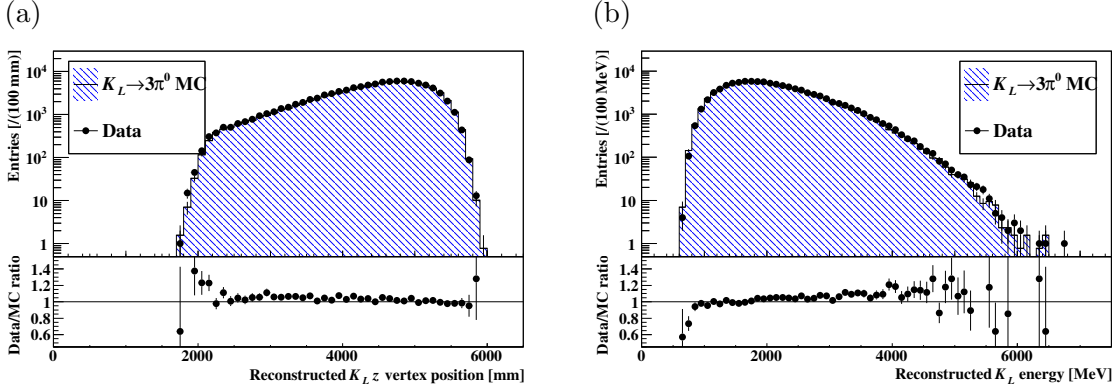


Fig. 4 Distributions of reconstructed K_L decay vertex position (a) and energy (b) of the $K_L \rightarrow 3\pi^0$ events. The bottom regions in both panels show the ratio of data and MC events for each histogram bin.

6. *Normalization* The number of observed events was normalized to the total number of the K_L decays in the collected data, which was obtained from the $K_L \rightarrow 2\pi^0$ decay events in the normalization data. We calculated the single event sensitivity (SES), which corresponds to the branching fraction with which we expect one signal event, as

$$\text{SES} = \frac{1}{A_{\text{sig}}} \frac{A_{\text{norm}} \text{Br}(K_L \rightarrow 2\pi^0)}{p N_{\text{norm}}},$$

where A_{sig} (A_{norm}) is the acceptance for the $K_L \rightarrow \pi^0 \nu \bar{\nu}$ ($K_L \rightarrow 2\pi^0$) decay, $\text{Br}(K_L \rightarrow 2\pi^0)$ is the branching fraction of the $K_L \rightarrow 2\pi^0$ decay [33], p is the prescale factor of 30 used to collect the $K_L \rightarrow 2\pi^0$ events, and N_{norm} is the number of observed $K_L \rightarrow 2\pi^0$ events in the data. The acceptance was defined as the efficiency that two (four) photons from the $K_L \rightarrow \pi^0 \nu \bar{\nu}$ ($K_L \rightarrow 2\pi^0$) decay were detected by the calorimeter, reconstructed as the K_L decay, and passed all the cuts. Using the acceptance ratio between the $K_L \rightarrow \pi^0 \nu \bar{\nu}$ and $K_L \rightarrow 2\pi^0$ decay modes reduced systematic uncertainties. The acceptances for $K_L \rightarrow \pi^0 \nu \bar{\nu}$

Table 2 Systematic uncertainties in the single event sensitivity.

source	relative uncertainty [%]
K_L momentum spectrum	± 1.51
photon selection cut	± 1.07
kinematic cuts for $K_L \rightarrow 2\pi^0$	± 2.46
kinematic cuts for $K_L \rightarrow \pi^0\nu\bar{\nu}$	± 2.81
cluster-shape-related cuts	± 2.51
veto cuts	± 5.50
L2 trigger effect	± 6.56
MC statistics	± 0.78
$K_L \rightarrow 2\pi^0$ branching fraction [33]	± 0.69
total	± 9.9

and $K_L \rightarrow 2\pi^0$ were evaluated with MC as $A_{\text{sig}} = 1.02\%$ and $A_{\text{norm}} = 0.59\%$. Based on the 1296 reconstructed $K_L \rightarrow 2\pi^0$ events within ± 15 MeV/ c^2 of the K_L mass peak shown in Fig. 3 (b), the SES was obtained to be $(1.28 \pm 0.04_{\text{stat.}} \pm 0.13_{\text{syst.}}) \times 10^{-8}$. This value is comparable to the final sensitivity of the E391a experiment, which was derived with a number of POT of 2.5×10^{18} with 12-GeV protons over four months [6].

Systematic uncertainties in SES are summarized in Table 2. The major uncertainties came from the veto cuts and the L2 trigger effect. The uncertainty in the veto cuts was evaluated by comparing the extra-particle rejection factors, defined as $N_{\text{all}}/N_{\text{cut}}$, of each veto counter between data and MC, where N_{all} is the number of events after imposing all the cuts, and N_{cut} is the number of events with all the cuts except a specific one. The $K_L \rightarrow 2\gamma$ decay instead of $K_L \rightarrow \pi^0\nu\bar{\nu}$ was used for the signal acceptance. The BCV veto cut showed the largest uncertainty of 4.0%. The uncertainty in the L2 trigger effect was due to trigger bias that remained after the offline COE cut was imposed. It did not affect the $K_L \rightarrow 2\pi^0$ acceptance because the L2 trigger was not used for the normalization data. The uncertainty was evaluated by studying the L2 efficiency as a function of the reconstructed COE value in the offline analysis from data samples with various trigger requirements and cuts. This uncertainty was found to be the largest, 6.56%.

7. Results After all the selection criteria were determined, the events in the signal region were examined. One event was observed as shown in Fig. 2. The number is consistent with with the expected number of background events summarized in Table 1. Assuming Poisson statistics with the statistical and systematic uncertainties considered [34], the 90% C.L. upper limit on $\text{Br}(K_L \rightarrow \pi^0\nu\bar{\nu})$ was set to be 5.1×10^{-8} .

We also studied the $K_L \rightarrow \pi^0 X^0$ decay suggested in Ref. [9, 10]. The same selection criteria as the $K_L \rightarrow \pi^0\nu\bar{\nu}$ search were used. The acceptance was evaluated and the corresponding upper limit was obtained for each X^0 mass. Figure 5 shows the 90% C.L. upper limit for the $K_L \rightarrow \pi^0 X^0$ decay as a function of the X^0 mass; we set an upper limit $\text{Br}(K_L \rightarrow \pi^0 X^0) < 3.7 \times 10^{-8}$ at the 90% C.L. for the X^0 mass of 135 MeV/ c^2 . This is the first result by a direct search for this process. It also improves the indirect limit obtained by scaling the limit given by the BNL E949 experiment, $\text{Br}(K^+ \rightarrow \pi^+ X^0) < 5.6 \times 10^{-8}$ [7], by a factor 6.5.

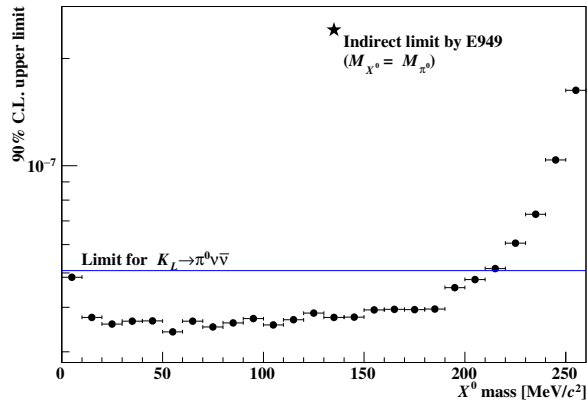


Fig. 5 Upper limit at the 90% C.L. on the $K_L \rightarrow \pi^0 X^0$ branching fraction as a function of the X^0 mass. For comparison, the limit on the $K_L \rightarrow \pi^0 \nu \bar{\nu}$ decay is shown with the blue line and the indirect limit by the E949 experiment with the star mark.

8. *Conclusions and prospects* Based on the 100-hour data taken with a 24-kW beam power in the first physics run in 2013, we set an upper limit on $\text{Br}(K_L \rightarrow \pi^0 \nu \bar{\nu})$ as 5.1×10^{-8} at the 90% C.L. and on $\text{Br}(K_L \rightarrow \pi^0 X^0)$ as 3.7×10^{-8} at the 90% C.L. for the X^0 mass of $135 \text{ MeV}/c^2$. This is the first direct search for the $K_L \rightarrow \pi^0 X^0$ process. Our result improves a previous indirect bound by a factor of 6.5 for $m_X = m_{\pi^0}$.

Since 2013, we have upgraded several detector subsystems to reduce K_L backgrounds [35, 36], and in 2015, we collected 20 times more data than what is reported in this letter. We also developed new analysis methods to discriminate photons from neutrons based on shower cluster shape [20] and waveform of hit crystals [37]. We are also preparing to modify the calorimeter to add a neutron discrimination capability [38]. With these improvements, we expect to suppress the neutron background sufficiently for the future results.

Acknowledgements

We would like to express our gratitude to all members of the J-PARC Accelerator and Hadron Experimental Facility groups for their support. We also thank the KEK Computing Research Center for KEKCC and National Institute of Information for SINET4. This material is based upon work supported by the Ministry of Education, Culture, Sports, Science, and Technology (MEXT) of Japan and the Japan Society for the Promotion of Science (JSPS) under the MEXT KAKENHI Grant Number JP18071006, the JSPS KAKENHI Grant Number JP23224007 and through the Japan-U.S. Cooperative Research Program in High Energy Physics; the U.S. Department of Energy, Office of Science, Office of High Energy Physics, under Award Numbers DE-SC0006497, DE-SC0007859, and DE-SC0009798; the Ministry of Education, the National Science Council/Ministry of Science and Technology in Taiwan under Grant Numbers 99-2112-M-002-014-MY3 and 102-2112-M-002-017; and the National Research Foundation of Korea (2012R-1A2A2A004554, 2013K1A3A7A06056592(Center of Korean J-PARC Users), and 2015R1A2A1A15056254). Some of the authors were supported by Grants-in-Aid for JSPS Fellows.

References

- [1] L. S. Littenberg, Phys. Rev. D **39**, 3322 (1989).
- [2] V. Cirigliano, G. Ecker, H. Neufeld, A. Pich and J. Portolés, Rev. Mod. Phys. **84**, 399 (2012), and references therein.
- [3] M. Tanimoto and K. Yamamoto, Prog. Theor. Exp. Phys. **2015**, 053B07 (2015).
- [4] A. J. Buras, D. Buttazzo and R. Knegjens, J. High Energy Phys. **1511** 166 (2015).

-
- [5] A. J. Buras, D. Buttazzo, J. Girrbach-Noe and R. Kneijens, *J. High Energy Phys.* **1511** 033 (2015).
- [6] J. K. Ahn *et al.* (E391a Collaboration), *Phys. Rev. D* **81**, 072004 (2010).
- [7] A. V. Artamonov *et al.* (E949 Collaboration), *Phys. Rev. D* **79**, 092004 (2009).
- [8] Y. Grossman and Y. Nir, *Phys. Lett. B* **398**, 163-168 (1997).
- [9] K. Fuyuto, W.-S. Hou and M. Kohda, *Phys. Rev. Lett.* **114**, 171802 (2015).
- [10] K. Fuyuto, W.-S. Hou and M. Kohda, *Phys. Rev. D* **93**, 054021 (2016).
- [11] T. Yamanaka, *Prog. Theor. Exp. Phys.* **2012**, 02B006 (2012).
- [12] S. Nagamiya, *Prog. Theor. Exp. Phys.* **2012**, 02B001 (2012).
- [13] K. Agari *et al.*, *Prog. Theor. Exp. Phys.* **2012**, 02B008 (2012).
- [14] T. Koseki *et al.*, *Prog. Theor. Exp. Phys.* **2012**, 02B004 (2012).
- [15] H. Takahashi *et al.*, *J. Radioanal. Nucl. Chem.* **305** 803-809 (2015).
- [16] T. Shimogawa, *Nucl. Instrum. Methods A* **623**, 585-587 (2010).
- [17] K. Shiomi, *Nucl. Instrum. Methods A* **664**, 264-271 (2012).
- [18] K. Sato *et al.*, *JPS Conf. Proc.* **8**, 024007 (2015).
- [19] T. Masuda *et al.*, *Nucl. Instrum. Methods A* **746**, 11-19 (2014).
- [20] E. Iwai *et al.*, *Nucl. Instrum. Methods A* **786**, 135 (2015).
- [21] T. Matsumura *et al.*, *Nucl. Instrum. Methods A* **795**, 19-31 (2015).
- [22] D. Naito *et al.*, *Prog. Theor. Exp. Phys.* **2016**, 023C01 (2016).
- [23] Y. Tajima *et al.*, *Nucl. Instrum. Methods A* **592**, 261-272 (2008).
- [24] N. Kawasaki, *Proc. Sci.*, KAON13 (2013) 040.
- [25] Y. Maeda *et al.*, *Prog. Theor. Exp. Phys.* **2015**, 063H01(2015).
- [26] M. Bogdan, J.-F. Genat, and Y. W. Wah, *Proc. 17th IEEE NPSS Real Time Conference*, 443-445 (2009).
- [27] M. Bogdan, J.-F. Genat, and Y. W. Wah, *Proc. 17th IEEE NPSS Real Time Conference*, 1-2 (2010).
- [28] M. Baba, *JPS Conf. Proc.* **8**, 051006 (2015).
- [29] Y. Sugiyama *et al.*, *IEEE Trans. Nucl. Sci.*, **62**, 1115-1121 (2015).
- [30] T. Masuda *et al.*, *Prog. Theor. Exp. Phys.* **2016**, 013C03 (2016).
- [31] Y. Maeda, Ph.D. thesis, Kyoto University (2016) (Available at: <http://www-he.scphys.kyoto-u.ac.jp/theses>, date last accessed September 5, 2016).
- [32] S. Agostinelli *et al.*, *Nucl. Instrum. Methods A* **506**, 250-303 (2003),
- [33] K. A. Olive *et al.* (Particle Data Group), *Chin. Phys.* **C38**, 090001 (2014).
- [34] R. D. Cousins and V. L. Highland, *Nucl. Instrum. Methods A* **320**, 331-335 (1992).
- [35] S. Shinohara, *Proc. Sci.*, FPCP2015 (2016) 079.
- [36] M. Togawa, *J. of Phys.: Conf. Ser.* **556** 012046 (2014).
- [37] Y. Sugiyama, Ph.D. thesis, Osaka University (2016) (Available at: <http://osksn2.hep.sci.osaka-u.ac.jp/theses/doctor.html>, date last accessed September 5, 2016).
- [38] K. Nakagiri, presentation in the International Conference on Kaon Physics 2016.